ORIGINAL ARTICLE

Estimating load in running: proposal of a novel simulation method.

Sebastian Deisting Skejø[a]

[a]Department of Health Science and Technology, Aalborg University

ARTICLE HISTORY
Compiled January 4, 2019

ABSTRACT
Running is a popular activity, but also an activity associated with a high incidence of injuries. In order to properly understand the aetiology of running, methods that can estimate the load of specific bodily structures, such as ligaments and muscles, in large, outdoor studies are needed. A novel simulation method based on a parametric statistical model of running and optimization of a few easily obtainable kinematic and anthropometric measures, is proposed. A candidate optimization objective was found using one set of data and the validity of the candidate objective in terms of sagital plane kinematics and kinetics was assessed in another set of data. In both data sets, there were poor agreement between the measured and the simulated kinematic and kinetic parameters. The most likely explanation for the lack of agreement was an insufficient setup of the optimization procedure, such as not using a full kinematic model in the optimization.

KEYWORDS
Running biomechanics, statistical modeling, musculoskeletal modeling, optimization

1. Introduction

Running is an immensely popular form of physical activity (Bueno et al. 2018) and participating in running is associated with health-related benefits (Lee et al. 2014; Hespanhol Junior et al. 2015). However, many runners sustain injuries (Videbæk et al. 2015), which is a primary reason for discontinuation of running (Koplan et al. 1995; Fokkema et al. 2019). Therefore, it is important to understand why running injuries occur and how they can be prevented. Risk factors of running injuries have been the focus of many studies (Hulme et al. 2017). However, in order to get a deeper understanding of why such injuries occur, running injury studies should be complemented with measurements or estimations of structure-specific loads, e.g. joint contact, ligament and muscle forces (Bertelsen et al. 2017). Measurements of structure-specific loads require highly invasive measurements techniques, such as implanting strain gauges in the ligaments and tendons (Ravary et al. 2004), but they can be estimated using musculoskeletal models (Marra et al. 2015). One approach is to use so-called inverse dynamics with muscle recruitment, which requires measurements of running kinematics and external loads. Both kinematics and external loads are typically measured in a lab equipped with a 3D motion capture system and force plates. However, when the kinematics of a runner are known, the external loads can be computed from the Newton-Euler equations of motion. Previous studies have shown that this approach to finding the external loads gives accurate estimations (Fluit et al. 2014; Skals et al. 2017). Therefore, only the kinematics of the runner are needed in order to obtain estimations of structure-specific loads. Nonetheless, for activities that are typically performed outdoors and in varying terrains, such as running, the requirement of being inside a lab poses a serious limitation. As such, methods that can measure or estimate running kinematics outside the lab are needed.

Running kinematics can be difficult to measure without the use of a lab. Recent development in wearable technology such as the Xsens MVN systems has enabled researchers to measure kinematics in settings outside the lab, such as during marathon running (Reenalda et al. 2016). However, such devices typically have a limited recording time (10 minutes in the case of Xsens MVN Link), and thus requires that another recording device is nearby. In the study by Reenalda et al. (2016) this limitation was solved by placing the external recording devices on bicycles, which followed the runners throughout the marathon. This solution appear infeasible for running injury studies, which typically require many participants followed over a long period of time in order to reduce the risk of bias (Nielsen et al. 2019). Therefore, kinematics should preferably be obtained in such a way that participants can manage the recording without the help of others. Such a method, might be offered by modern GPS-watches, which typically estimate several kinematic parameters, when used in conjuction with a chest belt. Kinematic parameters, that can be estimated this way include vertical oscillation of centre of mass, ground contact time and running velocity. Studies have shown that the estimation of these parameters is accurate (Adams et al. 2016; Watari et al. 2016). While the parameters available with the use of a GPS-watch are not enough to estimate the full-body kinematics, when used in isolation, kinematic parameters are often interrelated. For instance, Brughelli et al. (2011) found that as running velocity increases, vertical oscillation and ground contact time decreases. Further information relating to the runner, can be easily obtained by simple methods such as measuring weight, height and segment lengths. Thus, it can be speculated that if the relationships between the different kinematic and anthropometric parameters can be uncovered, it might be possible to estimate the entire full-body kinematics using only measurements from a GPS-watch.

Statistical modeling offers a way to express relationships between the different kinematic and anthropometric variables of interest. By measuring kinematics of a large sample of runners, a parametric statistical model of the measured variations of running can be constructed, which allows the variation in running patterns to be described by only a few parameters. Parametric models of running have been investigated in previous studies (Phinyomark et al. 2015; Clermont et al. 2017) and most recently in a master's thesis (Kloster and Iversen 2017). In the parametric model developed by Kloster and Iversen (2017), only 12 parameters were needed to describe more than 90% of the variation in the measured running patterns. However, the parametric model developed by Kloster and Iversen (2017) can not only describe the variation in running patterns. If instead of using the parameters as outputs of the statistical model, the values of the model parameters are assumed and used as input to the statistical model, the model can be used to generate new running patterns that maintain the relationships described by the parametric model. If a set of parameter values can be found such that the generated running pattern have the same characteristics as a measured running pattern, i.e. the same vertical oscillation, running velocity and ground contact time, it can be speculated that the generated and the measured running patterns might not just share characteristics, but also match in terms of the overall kinematics. However, obtaining the right set of parameters can be a difficult task given the (theoretically) infinite number of possible parameter values. One way to solve this is to use optimization. Using optimization, the parameter values are chosen in a systematic way such that the difference between the generated and the measured characteristics - vertical oscillation, running velocity and ground contact time - is minimized with as few guesses as possible.

Therefore, the purpose of this paper is to investigate whether sagital plane kinematics and kinetics of measured running can be accurately estimated by optimizing the parameters of a statistical model of running, using only measurements of vertical oscillation, running velocity, ground contact time and anthropometrics.

2. Materials and methods

Optimization is at the core of the approach taken in this study. In general, a typical aim of optimization is to minimize an objective function by systematically changing the input to the objective function. More specifically, in this study the aim was to minimize an objective function representing the difference between a measured and a simulated running pattern. The input to the objective function was the parameters of a statistical model based on principal components analysis (PCA) and the target characteristics of a measured running pattern. Thus, during each objective function evaluation, a simulated running pattern was generated by performing inverse PCA using the input parameters and characteristics of the simulated running pattern were compared to the target characteristics. Several sets of characteristics were used, but three kinematic parameter were present in all sets: vertical oscillation of centre of mass, running velocity and ground contact time. Other characteristics used in some versions of the objective functions were average vertical position of the centre of mass and length of the lower limb segments. Additionally, in some versions of the objective function, constraints were imposed, meaning that the simulated running patterns had to have certain traits, namely that the foot had to be in contact with the ground and that the kinematics could not result in simulated leg lengths that were longer than the measured leg length. All objective function used will be thoroughly described later.

In order to reduce bias resulting from using multiple different objective functions, running patterns were first generated using all the different objective functions and target characteristics of one set of data, and then the objective function which had the best performance, was used to generate running patterns matching another set of data. In the following, the statistical model, the two additional data set and the optimization procedure is thoroughly described.

2.1. Statistical model

A statistical model of running developed as part of a recent master's thesis was kindly provided to us. The method used to obtain the model is thoroughly described elsewhere (Kloster and Iversen 2017), but will be shortly summarized here.

The statistical model was based on 69 3-D motion capture and force plate recordings of running. The 69 recordings were reconstructed in the AnyBody Modeling System (AMS; AnyBody Technology A/S, Aalborg Denmark) using the MoCap Model Runner-model from the AnyBody Managed Model Repository (AMMR) version 1.6.3. This step included a) optimizing marker placement and segment dimensions, b) standardising the running direction, c) fixating the anteroposterior position of the pelvis in the lab coordinate system (i.e. simulating treadmill running) and in some cases, d) imputing joint angle time series for a half stride cycle as some recordings only had recorded data for a half stride cycle. The model had the joint positions of the wrist and neck fixed in a constant position leaving 30 degrees of freedom.

For each degree of freedom in the model, an FS approximation was derived in the sine-cosine form:

$$\theta_{\mathrm{i}} = A_0 + \sum_{\mathrm{i}=1}^{I} \left(A_{\mathrm{i}} \cos(\mathrm{i}\omega t) + B_{\mathrm{i}} \sin(\mathrm{i}\omega t)\right) \tag{1}$$

where I is the number of FS terms, A_{i} and B_{i} are the FS coefficients and ω is the frequency expressed in $\mathrm{rad\,s^{-1}}$.

The number of FS terms were chosen individually for each degree of freedom based on the correlation between the measured time series driving a degree of freedom and its FS. Next, FSs were phase shifted to ensure that the right heel strike happened at $t = 0$. In order to ensure that the feet would reach the ground, an FS driving the vertical position of the heel was included in the model. Similarly, an FS driving the anteroposterior position of the toes was included. The position of the model in relation to the ground coordinate system, was expressed by FSs for the x-, y- and z-position of the centre of mass for the entire model. The pelvis orientation was determined using FSs for each segment rotation and the remaining degrees of freedom were driven by joint angle FSs (for detailed information, see Kloster and Iversen (2017)). Finally, FSs were bilaterally averaged to enforce a symmetric running pattern and the left side FSs were constructed by phase shifting the right side FSs by half a period.

Measurements of trunk, upper and lower arm, shank, thigh and foot length as well as pelvis width, ω and all FS coefficients, were used as input for a PCA. This step was taken in order to discern the relationship between the different input variables and thus provide a basis for describing the most important variation in the measured running patterns with a limited number of parameters. The accepted level of explained variance was set at 95% which was achieved by using 16 principal components.

2.2. Motion capture models

Besides the data set used as input to the PCA, two sets of data were used. Set 1 (the training set) was used to tune the optimization procedure and select the best optimization setup. Set 2 (the validation set) was used the estimate the validity of the model. This approach was chosen as a mean to limit bias resulting from the initial process of tuning the optimization procedure.

Training set

The training set consisted of trials from two experienced runners (Runner 1: 28 years, 79.0 kg, 1.78 m; Runner 2: 39 years, 76.8 kg, 1.88 m). All trials were performed on an instrumented treadmill (M-Gait; Motekforce Link Amsterdam, The Netherlands) and kinematics was recorded by an active marker motion capture system (CX1; CODAmotion, Charnwood Dynamics, UK). Before warming up, subjects were weighed and measured. Following warm up, consisting of running at a self-selected pace on the treadmill, a static calibration trial was recorded. Then, runners performed trials at speeds of 10, 12, 14, 16 and 18 km/h with each trial lasting 60 seconds. There were no breaks between trials, but runners were given a 30-second accustomisation period before recording at each speed, implying that participants ran at each speed for a total of 90 seconds.

Marker positions and force plate recordings were imported into AMS and low-pass filtered using a fourth-order, zero-phase Butterworth filter with a cutoff frequency of 15 Hz. The AnyMoCap model from AMMR version 7.1 (similar to the Linearly scaled model of Lund et al. (2015)) without muscles was scaled using to each participant using the static calibration trial. The scaling was achieved by optimizing segment lengths and marker locations of markers not placed on anatomical landmarks based on a least-squares criterion (Andersen et al. 2010). Marker positions of the first two seconds of each running trials were then used to drive the scaled model by minimizing the least-squares difference between model and experimental markers (Andersen et al. 2009) and inverse dynamics analysis was performed.

Validation set

The validation set consisted of data collected as part of another research project (Skals et al. 2017). Ten healthy participants (eight males and two females, age 25.7±1.5 years, height 180.8±7.4 cm, weight 76.9±10.4 kg) took part in the study. Following warm up, participants performed several practice trials in order to familiarize themselves with the trial procedure and to establish a point from which they would start their runs. Four other types of movements were included in the original study (backwards running, a side-cut maneuver, vertical jump and acceleration from a standing position), but for brevity only the information relevant to the running trials are included here. Furthermore, all running trials were completed before the other types of movements.

Participants were instructed to run at a comfortable, self-selected pace and hit the force plate with the right foot without targetting. Following the practice trials, 35 reflective markers were placed on the participants, allowing trunk, lower and upper limb kinematics to be reconstructed. Marker trajectories were recorded using eight infrared high-speed cameras (Oqus 300 series) sampling at 250 Hz. Ground reaction forces and moments were recorded at 2000 Hz using a force plate (Advanced Mechanical Technology, Inc., Watertown, MA, US) embedded in the lab floor.

Three running trials were recorded per participant, giving a total of 30 validation trials. Each recording was cropped to only contain the stance phase and the surrounding few frames. Marker positions and ground reaction forces and moments were imported into AMS and marker positions were low-pass filtered using a fourth-order, zero-phase Butterworth filter with a cutoff frequency of 15 Hz. The marker positions from a walking trial were used to scale and optimize model marker positions of the GaitFullBody template from AMMR version 1.6.3 according to the procedure described by Andersen et al. (2010) Finally, kinematics and net joint moments were obtained by performing inverse dynamics analysis.

2.3. Optimization procedure

The input to the optimization objective was the parameters of the statistical model, i.e. the eigen values of the PCA. Five candidate optimization objectives were evaluated on the training set in order to find the best optimization procedure. The MINIMAL objective included only the three main parameters of the optimization, which were vertical oscillation of centre of mass (z_{VO}), running velocity (v) and ground contact time (t_{GCT}). The COMZ setup was similar to the minimal objective, but also optimized the mean vertical position of the centre of mass ($\bar{z}_{\text{CoM}}$) to match the $\bar{z}_{\text{CoM}}$ of subjects with

Parameters	Training set	Validation set	Objective
z_{VO}	Difference between maximum and minimum height of centre of mass	As in training set	As in training set
v	Minimum AP velocity of foot	Mean AP velocity of centre of mass	As in training set
t_{GCT}	Duration of foot contact measured with force plate	As in training set	Time from when heel drops below 4 cm until heel rises above 18 cm from the ground
$\bar{z}_{\mathrm{CoM}}$	Mean vertical centre of mass for subjects with similar segment lengths in the staticial model	As in training set	Mean vertical centre of mass
l_{thigh}	Measured in static trial	Optimized from walking trial	Reconstructed from inverse PCA
l_{shank}	Similarly to l_{thigh}	As in training set	As in training set
l_{foot}	Similarly to l_{thigh}	As in training set	As in training set
w_{pelvis}	Similarly to l_{thigh}	As in training set	As in training set

Table 1.: Computation of optimization parameters in the training and validation sets as well as in the objective. AP = anteroposterior.

similar segment lengths. This was achieved by constructing a linear model with $\bar{z}_{\mathrm{CoM}}$ as the dependent variable and segment lengths as independent variable using the input data to the statistical model. Given the measured segment lengths, the target $\bar{z}_{\mathrm{CoM}}$ was then computed from the linear model. The ANTHROPOMETRY objective included the three main parameters as well as segment lengths of thigh, shank and foot (l_{thigh}, l_{shank} and l_{foot} respectively) and pelvis width (w_{pelvis}) in the optimization. The SINGLE objective was similar to the MINIMAL objective, but only the first principal component was retained from the PCA. Finally, the MATCHED objective was similar to the ANTHROPOMETRY setup, but instead of modifying the eigen values, the optimization found the best running pattern from amongst the 69 recordings used as input for the PCA.

The target values (indicated by subscript $_{\mathrm{target}}$) for the optimization parameters were computed from the training and validation sets. Similarly, optimization parameters were computed during each call to the objective function ($_{\mathrm{optim}}$) by reconstructing the FSs using inverse PCA. The computation of all parameters is described in table 1. Given that only kinematic values were available during the optimization, $t_{\mathrm{GCT,optim}}$ could not be directly computed. Instead $t_{\mathrm{GCT,optim}}$ was estimated as the time between heel strike, defined as the instant the vertical position of the heel dropped below 4 cm, and toe off, defined as the instant the heel rose above 18 cm again. The threshold values used for the detection of ground contact were estimated from the training set and will be further discussed in later sections.

In order to obtain kinematics, that could be solved by AMS, two constraints were imposed on the optimization in all setups except MATCHED. Firstly, the minimum vertical position of the heel, $z_{\text{heel,min}}$, was constrained to be equal to 0.01 m, forcing the foot to make contact to the ground. Secondly, the distance between centre of mass and the foot, $d_{\text{CoM}\rightarrow\text{foot}}$ was constrained such that the optimization was less likely to produce kinematics that would require leg lengths larger than those of the simulation model. As the actual positions of any single point on the foot were unavailable during the optimization, $d_{\text{CoM}\rightarrow\text{foot}}$ was computed by assuming that the anteroposterior (AP) position of the toes and the vertical position of the heel represented the sagital plane coordinates of single point. The validity of this assumption will be discussed later. Subsequently, $d_{\text{CoM}\rightarrow\text{foot}}$ was computed as the Euclidean distance between the centre of mass and the assumed position of the foot. The maximum allowable distance between centre of mass and foot, $d_{\text{CoM}\rightarrow\text{foot,max}}$, was estimated by constructing a linear model from the data set used as input for the PCA, with $d_{\text{CoM}\rightarrow\text{foot}}$ as the dependent variable and thigh, shank and foot length as independent variables. Using this linear model, $d_{\text{CoM}\rightarrow\text{foot,max}}$ was estimated using the segment lengths of the participants in the training and validation sets.

By describing the parameters used in a given setup by x_{i} where x_{i} for i $= 1 \ldots n$ corresponds to each parameter and n is the number of parameters, the optimization objective is expressed by the following equation:

$$\min \quad \sum_{i}^{n} \left(\frac{1}{2} (x_{\text{i,target}} - x_{\text{i,optim}} \right)^2 \tag{2}$$

$$s.t. \quad z_{\text{heel,min}} = 0.01\,\text{m} \tag{3}$$

$$d_{\text{CoM}\rightarrow\text{foot}} \leq d_{\text{CoM}\rightarrow\text{foot,max}} \tag{4}$$

The optimization was solved using adaptive particle swarm optimization (Zhi-Hui Zhan et al. 2009). The particle swarm consisted of 10,000 particles and a total of one million calls to the objective function was allowed for the training set optimization. Five million objective function calls were allowed for the validation set. The optimization was bounded to the mean ± two standard deviations interval of the principal components obtained in the PCA (for implementation, see Appendix 8).

After the optimization, the reconstructed FSs from the optimization solution were imported into AMS and used to drive a simulation model. The simulation model was setup similarly to the statistical model. Muscles were modeled with a constant strength that did not depend on muscle state (e.g. contraction velocity and fiber length). Muscles were recruited using a cubic recruitment criterion with no upper bound on muscle activity. All FS drivers were implemented as "soft" kinematic constraints and kinematics were solved using the over-determinate solver of AMS (Andersen et al. 2009). Ground reaction forces and moments were predicted using the method developed by Fluit et al. (2014) with the height limit for contact detection set at 0.04 m and the relative velocity limit between foot and force plate set to 2 m/s. Finally, inverse dynamics was performed.

2.4. Statistical analysis

Hip flexion, knee flexion and ankle plantarflexion angles and net joint moments as well as ground contact times were extracted from both the simulation model and the corresponding training or validation set model. In the training set, the median and range of objective values were found in order to assess the success of the optimization procedure and the agreement between the simulated and measured parameters was computed as the root mean square error (RMSE) of the time-normalized stance phases. The best candidate objective was chosen based on the objective values and the median RMSEs in the training set and used for optimizing the validation set. In the validation set, the validity of the generated running patterns was assessed using the median and range of RMSEs. Additionally, the median and range of differences in maximum and minimum values were computed in the validation set. For both data sets, the shape of the simulated and measured parameters were compared by computing Pearson's correlation coefficient (r). The absolute values of r were categorized as weak, moderate, strong, and excellent for $r \leq 0.35$, $0.35 < r \leq 0.67$, $0.67 < r \leq 0.90$, and $0.90 < r$, respectively as per the guidelines of Taylor (1990).

3. Results

3.1. Training set

Only the COMZ and SINGLE objectives resulted in solvable kinematics for all 10 trials, when imported into AMS for inverse dynamics analysis. MINIMAL produced solvable kinematics in 9 of 10 trials, MATCHED produced kinematics that could be solved by AMS in 6 of 10 trials and only in 2 out of 10 trials could the kinematics produced with ANTHROPOMETRY be solved. Medians and ranges of RMSEs, objective values and differences in stance time between simulation and measurement are summarized in table 2. Curves of simulations and measurements are shown in appendix 1–5.

In general, correlations were similar across objectives, with moderate to strong correlations for hip flexion moment (median r for the five objectives ranging from 0.56 to 0.72), weak to moderate correlations for knee flexion moment (median r ranging from 0.13 to 0.53) and weak to moderate correlation for ankle plantarflexion moment (median r ranging from 0.07 to 0.57). Strong to excellent correlations were found for hip flexion angle (median r ranging from 0.89 to 0.98), knee flexion angle showed weak to strong correlations (median r ranging from 0.07 to 0.82) and moderate to strong correlations were found for ankle plantarflexion angle (median r ranging from 0.48 to 0.79). Medians and ranges of the correlations are shown in appendix 6.

Given the small objective values and comparable performance in terms of RMSEs, MINIMAL was chosen as the best candidate objective.

3.2. Validation set

Solvable kinematics was generated in 26 of 30 trials. The median difference in stance time between simulation and measurement was 0.03 s (range [-0.10; 0.11]). Median and range of RMSEs, differences in maximum values, differences in minimum values and correlation coefficients are summarized in table 3, but overall, simulation and measurement showed poor agreement. A representative example of net joint moments and joint angles, is shown in figure 1 (comparisons for all trials are shown in Appendix 7).

4. Discussion

The purpose of this article was to investigate whether running kinematics and kinetics could be accurately predicted from a few parameters, obtainable in large-scale, outdoor

Measure	MINIMAL	COMZ	ANTHROPOMETRY	SINGLE	MATCHED
Objective value	3.7e−9 [7.9e−10; 9.7e−7]	3.4e−7 [9.8e−10; 7.6e−6]	5.6e−4 [2.7e−4; 1.1e−3]	0.27 [0.17; 0.89]	6.3e−3 [2.6e−3; 1.6e−2]
Difference in stance time (s)	-0.01 [-0.08; 0.06]	0.00 [-0.10; 0.04]	0.06 [0.02; 0.09]	0.00 [-0.01; 0.07]	-0.03 [-0.07; 0.05]
Hip flexion moment ($\mathrm{N\,m\,kg^{-1}}$)	1.4 [1.0; 1.6]	1.4 [0.9; 2.3]	1.9 [1.3; 2.6]	1.4 [1.1; 1.9]	1.4 [0.9; 1.9]
Knee flexion moment ($\mathrm{N\,m\,kg^{-1}}$)	0.9 [0.8; 2.4]	1.5 [0.7; 2.0]	1.1 [1.0; 1.1]	1.4 [0.9; 1.6]	1.5 [0.6; 1.8]
Ankle plantarflexion moment ($\mathrm{N\,m\,kg^{-1}}$)	0.9 [0.7; 1.3]	1.0 [0.5; 1.3]	0.8 [0.5; 1.0]	0.9 [0.5; 1.4]	1.1 [0.7; 1.5]
Hip flexion angle (°)	15.3 [3.8; 33.3]	22.4 [8.8; 30.3]	15.2 [3.2; 27.2]	8.4 [5.9; 15.0]	20.3 [15.0; 29.9]
Knee flexion angle (°)	33.7 [15.7; 50.8]	42.3 [36.9; 46.5]	19.4 [15.2; 23.6]	26.6 [16.7; 32.8]	39.9 [14.3; 46.5]
Ankle plantarflexion angle (°)	15.4 [7.6; 28.1]	16.6 [7.3; 24.8]	21.6 [19.8; 23.4]	14.7 [13.0; 18.7]	20.9 [18.0; 23.7]

Table 2.: Median and range of RMSEs for the five candidate objectives.

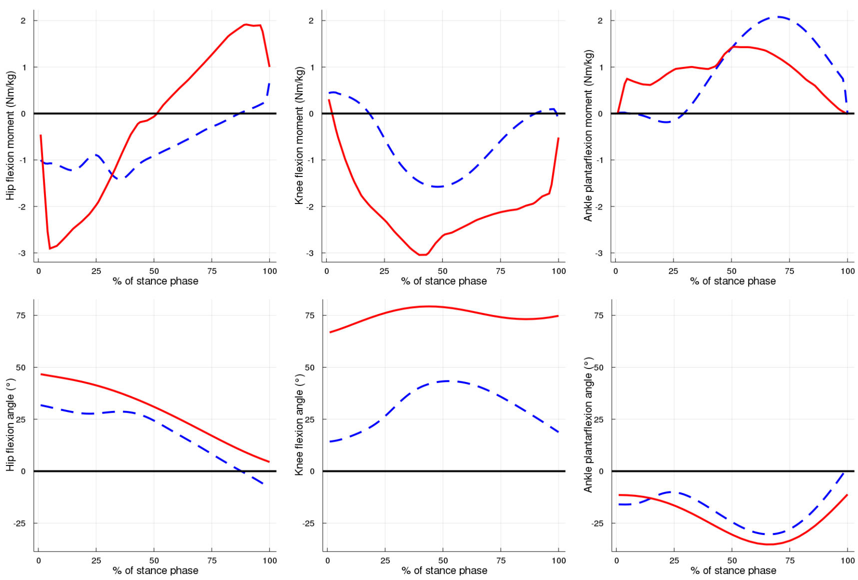

Figure 1.: A representative example of measured (blue dashed) and simulated (red solid) net joint moments and joint angles.

Measure	RMSE	Difference in minimum	Difference in maximum	Correlation coefficient (r)
Hip flexion moment ($\mathrm{N\,m\,kg^{-1}}$)	1.7 [0.4; 2.8]	-0.7 [-2.7; 1.2]	1.3 [-1.3; 3.9]	0.70 [-0.10; 0.95]
Knee flexion moment ($\mathrm{N\,m\,kg^{-1}}$)	1.2 [0.5; 2.7]	-0.2 [-3.2; 1.5]	0.0 [-0.7; 0.7]	0.56 [-0.11; 0.97]
Ankle plantarflexion moment ($\mathrm{N\,m\,kg^{-1}}$)	1.0 [0.5; 1.5]	0.0 [-0.3; 0.2]	-0.7 [-1.6; 0.0]	0.62 [-0.56; 0.92]
Hip flexion angle (°)	11.4 [1.7; 30.2]	7.1 [-22.6; 39.8]	9.2 [-14.0; 35.3	0.94 [0.85; 1.00]
Knee flexion angle (°)	31.0 [11.3; 54.2]	39.9 [15.1; 63.8]	22.7 [3.6; 46.2]	0.57 [-0.87; 0.96]
Ankle plantarflexion angle (°)	13.0 [2.9; 24.5]	-4.3 [-22.3; 9.2]	-2.1 [-30.0; 26.0]	0.65 [-0.58; 0.97]

Table 3.: Summary of median and ranges of RMSEs, differences in minimum and maximum values and correlation coefficients between simulation and measurement.

field studies of running injuries. Five different objectives were tested in the training set, with MINIMAL and COMZ resulting in small objective values, indicating succesful optimization. Furthermore, MINIMAL resulted in lower median RMSEs than COMZ for five of six kinematic and kinetic parameter and thus MINIMAL was chosen as the best candidate objective. Optimizing using MINIMAL in the validation set, results showed poor agreement between the simulation and the measurements as indicated by high RMSEs. Moderate to excellent median correlations were found between simulation and measurement in the validation set, however the ranges of the correlations were large. For instance, the correlations for the knee flexion angle ranged from -0.87 to 0.96.

While the proposed method did not work, to our knowledge, this study was the first to propose a method with the potential of being able to estimate kinematics and kinetics of the entire body. Other methods that do not require a 3D motion capture setup have been proposed to estimate some of the kinematic and kinetic parameters relevant to running. For instance, Wille et al. (2014) tried to estimate knee extensor moment and ground reaction forces as well as other kinetic parameters using sagital plane kinematics only. Their method had moderate succes with R^2 of the developed models ranging from 0.04 to 0.58. Another approach was taken by Wouda et al. (2018) who estimated ground reaction forces and knee joint angles using machine learning and inertial measurements units placed and the pelvis and both lower legs. Excellent agreement between the machine learning method and motion capture and force plate recordings was found, with the RMSE of the knee flexion angle ranging from 1.74 to 4.38° and RMSE of the vertical ground reaction force ranging from 0.12 to 0.33 body weights. Nonetheless, both of these approaches are limited in the sense that is only possible to estimate the kinematic and kinetic parameters explicitly included as outcomes. On the other hand, the method we proposed could have the potential to estimate the load of any structure given that the method is based on a full body musculoskeletal model which, combined with the advanced computational methods employed by AMS, can yield valid estimations of structure-specific loads (Fregly et al. 2012). Therefore it is worth considering why the proposed method showed bad performance and how improvements can be made.

There can be several explanations as to why the proposed method failed to produce valid results. One explanation could be that is simply not possible to generate a running pattern matching the targetted, from the statistical model. For example, if the input data to the PCA consisted of rearfoot running, it would be less likely that forefoot running could be accurately reproduced by the proposed method. While, we didn't have information regarding the footstrike patterns of the input data, we noted that the proposed method most often generated rearfoot running, suggesting that the input data did indeed consist mostly of rearfoot running. However, the validation data also consisted of rearfoot running and thus the lack of validity must likely be explained by other factors. On the other hand the training set consisted of both rearfoot and forefoot running, which could potentially have introduced some bias in the selection of the best objective. Nonetheless, it seems unlikely that this would be the case. Furthermore, the targetted vertical oscillation, running velocity and estimated ground contact time of the training and validation sets, where all within the range of the same parameters for the data used to construct the PCA. Therefore, it appears unlikely that the running patterns of the validation trials were so vastly different from the data used to create the statistical model, that the statistical model could not express the kinematics of the validation set.

Another explanation could be that the optimization procedure needs to be setup in a different way. While we partly explored this explanation by testing five different objectives, many other objectives could have been tried. The range of optimization parameters was severly limited by the fact that only some kinematic parameters were available during the optimization. This restriction was due to that fact that reaching convergence required many calls to the objective. Thus, it was not possible to use AMS to find kinetic values during each objective call as each AMS analysis would take several minutes to complete, increasing the total optimization time to infeasible lengths. However, it appears likely that including kinetic parameters in the optimization would produce better results. For instance, studies have found that humans tend to select gait parameters that minimize the metabolic cost (Alexander 1989; Gutmann and Bertram 2017; Bertram and Ruina 2001). Therefore, including a kinetic optimization parameter such as mechanical work performed, could potentially improve the optimization. Furthermore, only a limited amount of kinematic information was available during the optimization, namely the FSs used to control the kinematics. It is likely that a full kinematic model could aid the optimization as information, such as the exact position of a single point on the foot, would become available. However, in order to obtain such measures, a kinematic model of the entire body had to be constructed as the position of the model was partly determined by the position of the centre of mass. Implementing a full body kinematic model efficiently enough to be used during each objective function evaluation was well outside the scope of this project and performing the kinematic analysis in AMS would require several seconds of computation time for each objective function evaluation, which would make the optimization approach extremely time-consuming. Nonetheless, a full kinematics model might be a requisite for the proposed method to work and therefore future studies should investigate this possibility.

Another source of error might be the inequality constraint on the distance between centre of mass and the foot, which was necessary in order to achieve kinematics that would not require larger-than-measured segment lengths and thus could be solved by AMS. However, the imposed upper limit on the inequality constraint may have forced the optimization to produce suboptimal running patterns. The upper limit was computed from a linear model constructed from the input data. Thus, the distance between the foot and the centre of mass could never be above the recorded mean for the given segment lengths. Combined with the fact that the minimum vertical position of the heel was constrained, the inequality constraint could have caused the centre of mass to have been placed lower than it should have been. Such a limitation could likely show up as increased hip and/or knee flexion. Since the differences in both minimum and maximum hip and knee flexion angles were positive and thus indicating that the simulated flexion angles were larger than the measured flexion angles, it does indeed appear to be the case that the centre of mass was placed too low in the simulated running patterns. It seems likely that this limitation could be avoid if a full kinematic model had been used. Had a full kinematic model been used, the actual position of each segment would have been known and thus each segment length could have been constrained individually to the measured segment length.

Another potential issue with the optimization setup was the definition of ground contact time in the optimization objective. Since it wasn't possible to use AMS during the optimization, only kinematic variables were available as a mean to detect ground contact time. Other studies have developed methods to identify heel strike and toe off from kinematic data, but these methods rely on knowing both AP and vertical position for both the heel and the toes (Leitch et al. 2011; De Witt 2010; Zeni et al. 2008; Osis et al. 2014). Information regarding the AP position of the toes and the vertical position of the heel requires a full kinematic model, which was not available during the optimization, as discussed above. Therefore, we estimated the ground contact time by only considering the vertical position of the heel. The threshold values for heel strike and toe off were set at 0.04 and 0.18 m, respectively. These values were estimated from the training set, but it seems likely that the threshold values should be based on an individual assessment at least accounting for different lengths of the feet. Indeed, in the validation set heel strikes happened with vertical position of the heel ranging from 0.02 to 0.04 m and toe off happened with the heel positioned 0.08 to 0.19 m above the ground. However, as the training set consisted of only two participants and no information regarding ground contact was present in the input data to the PCA, no correction for individual variation was attempted. While there was good coherence between the ground contact time estimated during the optimization and the targetted ground contact time, when the simulation was performed in AMS the actual simulated ground contact time deviated significantly from the targetted ground contact time. The disagreement could likely be explained by the fact that the simulated ground contact also required that the velocity of the foot relative to the ground was below a threshold of 2 m/s. Thus, even though the foot was spatially in contact with the floor, if the foot was moving too fast, AMS would not recognize the foot contact. The velocity threshold is needed for AMS to correctly identify toe off as a failure to correctly identify toe off often leads to dynamically insolvable systems. While we did not rigorously test higher velocity thresholds, the few tests we completed indicated that higher threshold values led to the dynamics becoming insolvable by AMS. It should also be noted that the used threshold of 2 m/s was already 2.5 times larger than the default threshold of 0.8 m/s (Fluit et al. 2014). We also tried other methods for estimating ground contact time, such as constraining the foot velocity during the ground contact time estimated by the vertical heel position and by detecting heel strike and toe off based on both position and velocity of heel and toe, but the estimation based only vertical position of the heel appeared to give the best results. For instance, constraining the foot velocity, estimated by the AP velocity of the toes and the vertical velocity of the heel, to 2 m/s during ground contact still resulted in a median difference in ground contact time ranging -0.09 to 0.03 s, while RMSEs increased by an average of 10.3% in the training set. Furthermore, selecting a subset of the validation data, where the difference in ground contact time between simulation and measurement were close to zero (six trials with a

Measure	RMSE	Difference in minimum	Difference in maximum	Correlation coefficient (r)
Hip flexion moment ($\mathrm{N\,m\,kg^{-1}}$)	2.2 [0.9; 2.8]	-0.6 [-1.5; 0.6]	2.9 [1.2; 3.9]	0.83 [0.68; 0.93]
Knee flexion moment ($\mathrm{N\,m\,kg^{-1}}$)	1.5 [1.3; 2.7]	-1.0 [-3.2; -0.2]	-0.1 [-0.3; 0.0]	-0.02 [-0.11; 0.85]
Ankle plantarflexion moment ($\mathrm{N\,m\,kg^{-1}}$)	0.5 [0.5; 1.0]	0.1 [0.0; 0.2]	-0.4 [-1.5; 0.0]	0.85 [0.46; 0.92]
Hip flexion angle (°)	13.1 [3.7; 28.2]	9.5 [-16.5; 20.0]	0.1 [-5.4; 28.9]	0.94 [0.89; 0.99]
Knee flexion angle (°)	26.6 [17.6; 44.5]	38.3 [20.5; 52.5]	16.7 [3.6; 35.9]	0.57 [0.05; 0.84]
Ankle plantarflexion angle (°)	7.5 [6.5; 15.9]	-1.7 [-8.0; 9.2]	-9.8 [-13.0; 10.7]	0.90 [-0.21; 0.94]

Table 4.: Summary of median and ranges of RMSEs, differences in minimum and maximum values and correlation coefficients between simulation and measurement in a subset of the validation set data consisting of the six trials, that had a difference in ground contact time larger than -0.02 s and less than 0.02 s.

difference larger than -0.02 s and smaller than 0.02 s), did not improve the agreement between simulation and measurement (see Table 4). This is an indication that the definition of ground contact time in the objective function, is likely not the sole reason for the incoherence between simulations and measurements. Nonetheless, the lack of coherence between the estimated and simulated ground contact time is a significant problem with the employed method.

In addition to not giving valid estimations, the proposed method comes with a few limitations. As noted previously, the statistical model appeared to mostly produce rearfoot running. Therefore, even if a working optimization setup can be found, it is likely that the proposed method would have difficulties with accurately simulating forefoot running. The only way to work around this limitation is to include forefoot runners in the statistical model. Another limitation is the fact the simulated running pattern are always symmetric, while studies have shown that the asymmetry can be quite pronounced (Furlong and Egginton 2018; Zifchock et al. 2006). However, if the asymmetry can be measured, e.g. by measuring the ground contact time or similar kinematic variables for each step, it should be straightforward to modify the proposed method to account for asymmetry.

In conclusion, the proposed method of simulating full body kinematics on the basis of optimization of a few kinematic and anthropometric measures, did not produce valid estimations of sagital plane, lower limb kinematics and kinetics. Explanations for the discrepancies between simulations and measurement were most likely a result of errors in the optimization setup. Particularly, the fact that a full kinematic model was not available during the optimization, could be an important reason for the missing coherence.

References

Adams D, Pozzi F, Carroll A, Rombach A, Zeni J. 2016. Validity and Reliability of a Commercial Fitness Watch for Measuring Running Dynamics. Journal of Orthopaedic & Sports Physical Therapy. 46(6):471–476. Available from: http://www.jospt.org/doi/10.2519/jospt.2016.6391.

Alexander RM. 1989. Optimization and gaits in the locomotion of vertebrates. Physiological Reviews. 69(4):1199–1227. Available from: http://www.physiology.org/doi/10.1152/physrev.1989.69.4.1199.

Andersen M, Damsgaard M, MacWilliams B, Rasmussen J. 2010. A computationally efficient optimisation-based method for parameter identification of kinematically determinate and over-determinate biomechanical systems. Computer Methods in Biomechanics and Biomedical Engineering. 13(2):171–183. Available from: http://www.tandfonline.com/doi/abs/10.1080/10255840903067080.

Andersen MS, Damsgaard M, Rasmussen J. 2009. Kinematic analysis of over-determinate biomechanical systems. Computer Methods in Biomechanics and Biomedical Engineering. 12(4):371–384. Available from: http://www.tandfonline.com/doi/abs/10.1080/10255840802459412.

Bertelsen ML, Hulme A, Petersen J, Brund RK, Sørensen H, Finch CF, Parner ET, Nielsen RO. 2017. A framework for the etiology of running-related injuries. Scandinavian Journal of Medicine & Science in Sports. 27(11):1170–1180. Available from: http://doi.wiley.com/10.1111/sms.12883.

Bertram JE, Ruina A. 2001. Multiple Walking Speed–frequency Relations are Predicted by Constrained Optimization. Journal of Theoretical Biology. 209(4):445–453. Available from: http://linkinghub.elsevier.com/retrieve/pii/S0022519301922799.

Brughelli M, Cronin J, Chaouachi A. 2011. Effects of Running Velocity on Running Kinetics and Kinematics. Journal of Strength and Conditioning Research. 25(4):933–939. Available from: https://insights.ovid.com/crossref?an=00124278-201104000-00008.

Bueno AM, Pilgaard M, Hulme A, Forsberg P, Ramskov D, Damsted C, Nielsen RO. 2018. Injury prevalence across sports: a descriptive analysis on a representative sample of the Danish population. Injury Epidemiology. 5(1):6. Available from: https://injepijournal.springeropen.com/articles/10.1186/s40621-018-0136-0.

Clermont CA, Osis ST, Phinyomark A, Ferber R. 2017. Kinematic Gait Patterns in Competitive and Recreational Runners. Journal of Applied Biomechanics. 33(4):268–276. Available from: http://journals.humankinetics.com/doi/10.1123/jab.2016-0218.

De Witt JK. 2010. Determination of toe-off event time during treadmill locomotion using kinematic data. Journal of Biomechanics. 43(15):3067–3069. Available from: http://dx.doi.org/10.1016/j.jbiomech.2010.07.009 https://linkinghub.elsevier.com/retrieve/pii/S0021929010003908.

Fluit R, Andersen M, Kolk S, Verdonschot N, Koopman H. 2014. Prediction of ground reaction forces and moments during various activities of daily living. Journal of Biomechanics. 47(10):2321–2329. Available from: http://dx.doi.org/10.1016/j.jbiomech.2014.04.030 https://linkinghub.elsevier.com/retrieve/pii/S0021929014002516.

Fokkema T, Hartgens F, Kluitenberg B, Verhagen E, Backx FJ, van der Worp H, Bierma-Zeinstra SM, Koes BW, van Middelkoop M. 2019. Reasons and predictors of discontinuation of running after a running program for novice runners. Journal of Science and Medicine in Sport. 22(1):106–111. Available from: https://doi.org/10.1016/j.jsams.2018.06.003 https://linkinghub.elsevier.com/retrieve/pii/S1440244018302469.

Fregly BJ, Besier TF, Lloyd DG, Delp SL, Banks SA, Pandy MG, D'Lima DD. 2012. Grand challenge competition to predict in vivo knee loads. Journal of Orthopaedic Research. 30(4):503–513. Available from: http://doi.wiley.com/10.1002/jor.22023.

Furlong LAM, Egginton NL. 2018. Kinetic Asymmetry during Running at Preferred and Nonpreferred Speeds. Medicine & Science in Sports & Exercise. 50(6):1241–1248. Available from: http://insights.ovid.com/crossref?an=00005768-201806000-00015.

Gutmann AK, Bertram JEA. 2017. The apparently contradictory energetics of hopping and running: the counter-intuitive effect of constraints resolves the paradox. The Journal of Experimental Biology. 220(2):167–170. Available from: http://jeb.biologists.org/lookup/doi/10.1242/jeb.144832.

Hespanhol Junior LC, Pillay JD, van Mechelen W, Verhagen E. 2015. Meta-Analyses of the Effects of Habitual Running on Indices of Health in Physically Inactive Adults. Sports Medicine. 45(10):1455–1468. Available from: http://link.springer.com/10.1007/s40279-015-0359-y.

Hulme A, Nielsen RO, Timpka T, Verhagen E, Finch C. 2017. Risk and Protective Factors for Middle- and Long-Distance Running-Related Injury. Sports Medicine. 47(5):869–886. Available from: http://link.springer.com/10.1007/s40279-016-0636-4.

Kloster BV, Iversen K. 2017. Parameterizing Running Kinematics, MSc Thesis [dissertation]. Aalborg University.

Koplan JP, Rothenberg RB, Jones EL. 1995. The natural history of exercise. Medicine & Science in Sports & Exercise. 27(8):1180???1184. Available from: http://www.ncbi.nlm.nih.gov/pubmed/7476063 https://insights.ovid.com/crossref?an=00005768-199508000-00012.

Lee Dc, Pate RR, Lavie CJ, Sui X, Church TS, Blair SN. 2014. Leisure-Time Running Reduces All-Cause and Cardiovascular Mortality Risk. Journal of the American College of Cardiology. 64(5):472–481. Available from: https://linkinghub.elsevier.com/retrieve/pii/S0735109714027466.

Leitch J, Stebbins J, Paolini G, Zavatsky AB. 2011. Identifying gait events without a force plate during running: A comparison of methods. Gait & Posture. 33(1):130–132. Available from: http://dx.doi.org/10.1016/j.gaitpost.2010.06.009 https://linkinghub.elsevier.com/retrieve/pii/S0966636210001670.

Lund ME, Andersen MS, de Zee M, Rasmussen J. 2015. Scaling of musculoskeletal models from static and dynamic trials. International Biomechanics. 2(1):1–11. Available from: http://www.tandfonline.com/doi/full/10.1080/23335432.2014.993706.

Marra MA, Vanheule V, Fluit R, Koopman BHFJM, Rasmussen J, Verdonschot N, Andersen MS. 2015. A Subject-Specific Musculoskeletal Modeling Framework to Predict In Vivo Mechanics of Total Knee Arthroplasty. Journal of Biomechanical Engineering. 137(2):020904. Available from: http://biomechanical.asmedigitalcollection.asme.org/article.aspx?articleid=2108397 http://biomechanical.asmedigitalcollection.asme.org/article.aspx?doi=10.1115/1.4029258.

Nielsen RO, Bertelsen ML, Ramskov D, Møller M, Hulme A, Theisen D, Finch CF, Fortington LV, Mansournia MA, Parner ET. 2019. Time-to-event analysis for sports injury research part 2: time-varying outcomes. British Journal of Sports Medicine. 53(1):70–78. Available from: http://bjsm.bmj.com/lookup/doi/10.1136/bjsports-2018-100000.

Osis ST, Hettinga BA, Leitch J, Ferber R. 2014. Predicting timing of foot strike during running, independent of striking technique, using principal component analysis of joint angles. Journal of Biomechanics. 47(11):2786–2789. Available from: http://dx.doi.org/10.1016/j.jbiomech.2014.06.009 https://linkinghub.elsevier.com/retrieve/pii/S0021929014003480.

Phinyomark A, Osis S, Hettinga BA, Leigh R, Ferber R. 2015. Gender differences in gait kinematics in runners with iliotibial band syndrome. Scandinavian Journal of Medicine & Science in Sports. 25(6):744–753. Available from: http://doi.wiley.com/10.1111/sms.12394.

Ravary B, Pourcelot P, Bortolussi C, Konieczka S, Crevier-Denoix N. 2004. Strain and force transducers used in human and veterinary tendon and ligament biomechanical studies. Clinical Biomechanics. 19(5):433–447. Available from: http://linkinghub.elsevier.com/retrieve/pii/S0268003304000221.

Reenalda J, Maartens E, Homan L, Buurke JJ. 2016. Continuous three dimensional analysis of running mechanics during a marathon by means of inertial magnetic measurement units to objectify changes in running mechanics. Journal of Biomechanics. 49(14):3362–3367. Available from: http://dx.doi.org/10.1016/j.jbiomech.2016.08.032 https://linkinghub.elsevier.com/retrieve/pii/S002192901630968X.

Skals S, Jung MK, Damsgaard M, Andersen MS. 2017. Prediction of ground reaction forces and moments during sports-related movements. Multibody System Dynamics. 39(3):175–195. Available from: http://dx.doi.org/10.1007/s11044-016-9537-4

http://link.springer.com/10.1007/s11044-016-9537-4.
Taylor R. 1990. Interpretation of the Correlation Coefficient: A Basic Review. Journal of Diagnostic Medical Sonography. 6(1):35–39. Available from: http://journals.sagepub.com/doi/10.1177/875647939000600106.
Videbæk S, Bueno AM, Nielsen RO, Rasmussen S. 2015. Incidence of Running-Related Injuries Per 1000 h of running in Different Types of Runners: A Systematic Review and Meta-Analysis. Sports Medicine. 45(7):1017–1026. Available from: http://link.springer.com/10.1007/s40279-015-0333-8.
Watari R, Hettinga B, Osis S, Ferber R. 2016. Validation of a Torso-Mounted Accelerometer for Measures of Vertical Oscillation and Ground Contact Time during Treadmill Running. Journal of Applied Biomechanics. 32(3):306–310. Available from: http://journals.humankinetics.com/doi/10.1123/jab.2015-0200.
Wille CM, Lenhart RL, Wang S, Thelen DG, Heiderscheit BC. 2014. Ability of Sagittal Kinematic Variables to Estimate Ground Reaction Forces and Joint Kinetics in Running. Journal of Orthopaedic & Sports Physical Therapy. 44(10):825–830. Available from: http://www.jospt.org/doi/10.2519/jospt.2014.5367.
Wouda FJ, Giuberti M, Bellusci G, Maartens E, Reenalda J, van Beijnum BJF, Veltink PH. 2018. Estimation of Vertical Ground Reaction Forces and Sagittal Knee Kinematics During Running Using Three Inertial Sensors. Frontiers in Physiology. 9(MAR):1–14. Available from: http://journal.frontiersin.org/article/10.3389/fphys.2018.00218/full.
Zeni J, Richards J, Higginson J. 2008. Two simple methods for determining gait events during treadmill and overground walking using kinematic data. Gait & Posture. 27(4):710–714. Available from: http://linkinghub.elsevier.com/retrieve/pii/S0966636207001804.
Zhi-Hui Zhan, Jun Zhang, Yun Li, Chung HH. 2009. Adaptive Particle Swarm Optimization. IEEE Transactions on Systems, Man, and Cybernetics, Part B (Cybernetics). 39(6):1362–1381. Available from: http://ieeexplore.ieee.org/lpdocs/epic03/wrapper.htm?arnumber=4812104.
Zifchock RA, Davis I, Hamill J. 2006. Kinetic asymmetry in female runners with and without retrospective tibial stress fractures. Journal of Biomechanics. 39(15):2792–2797. Available from: http://linkinghub.elsevier.com/retrieve/pii/S0021929005004471.

Appendix 1: MINIMAL-simulations vs measurements

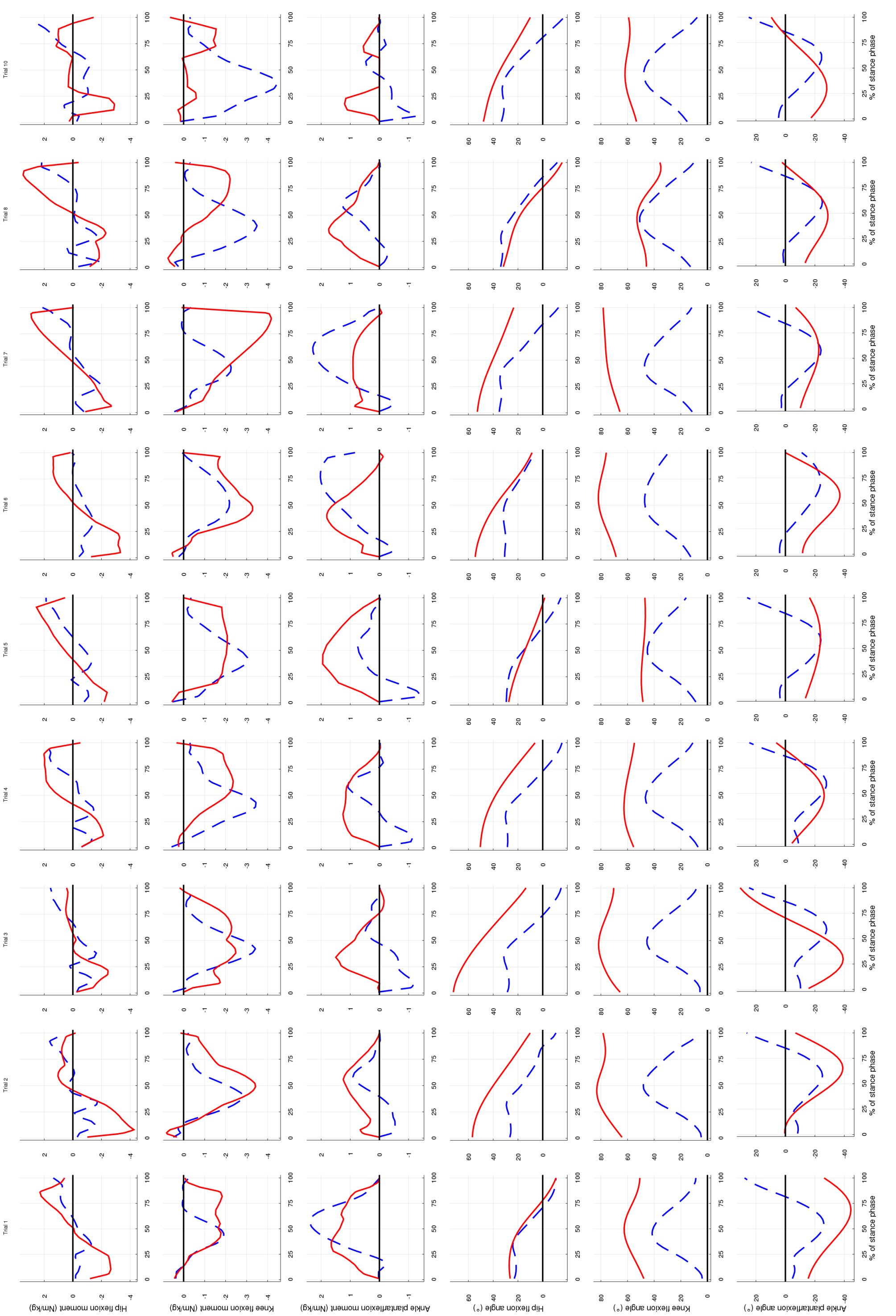

Figure 2.: Comparison of simulation results obtained with the MINIMAL objective (red solid) and measurements (blue dashed). Each column contains one trial and each row contains one parameter.

Appendix 2: COMZ-simulations vs measurements

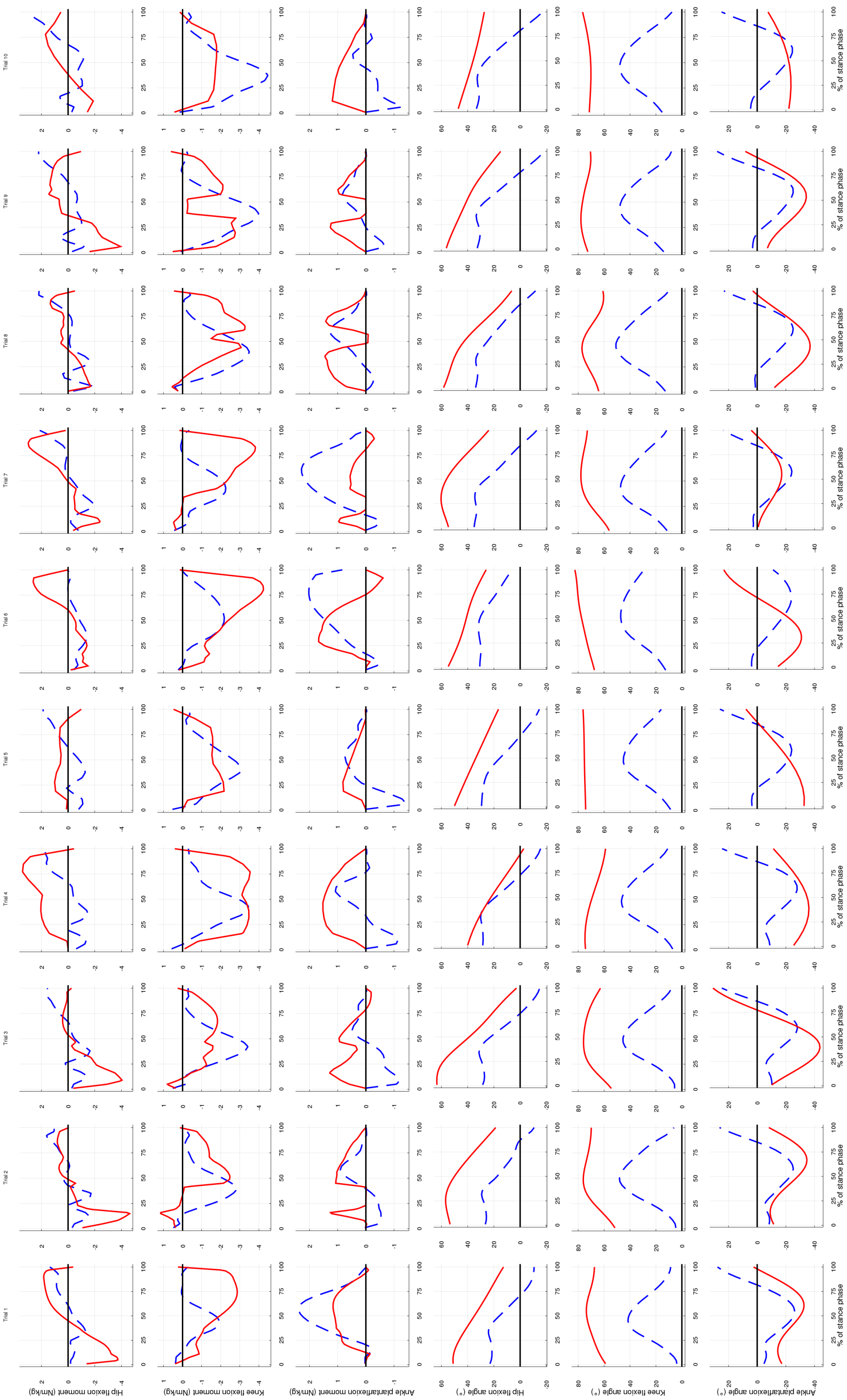

Figure 3.: Comparison of simulation results obtained with the COMZ objective (red solid) and measurements (blue dashed). Each column contains one trial and each row contains one parameter.

Appendix 3: ANTHROPOMETRY-simulations vs measurements

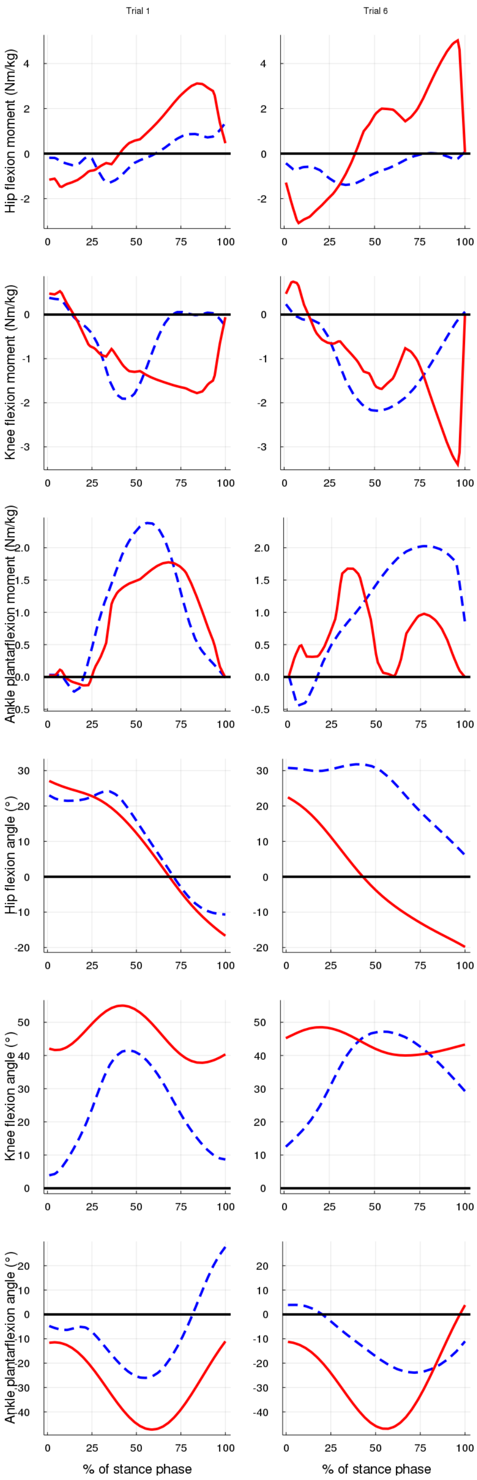

Figure 4.: Comparison of simulation results obtained with the ANTHROPOMETRY objective (red solid) and measurements (blue dashed). Each column contains one trial and each row contains one parameter.

Appendix 4: SINGLE-simulations vs measurements

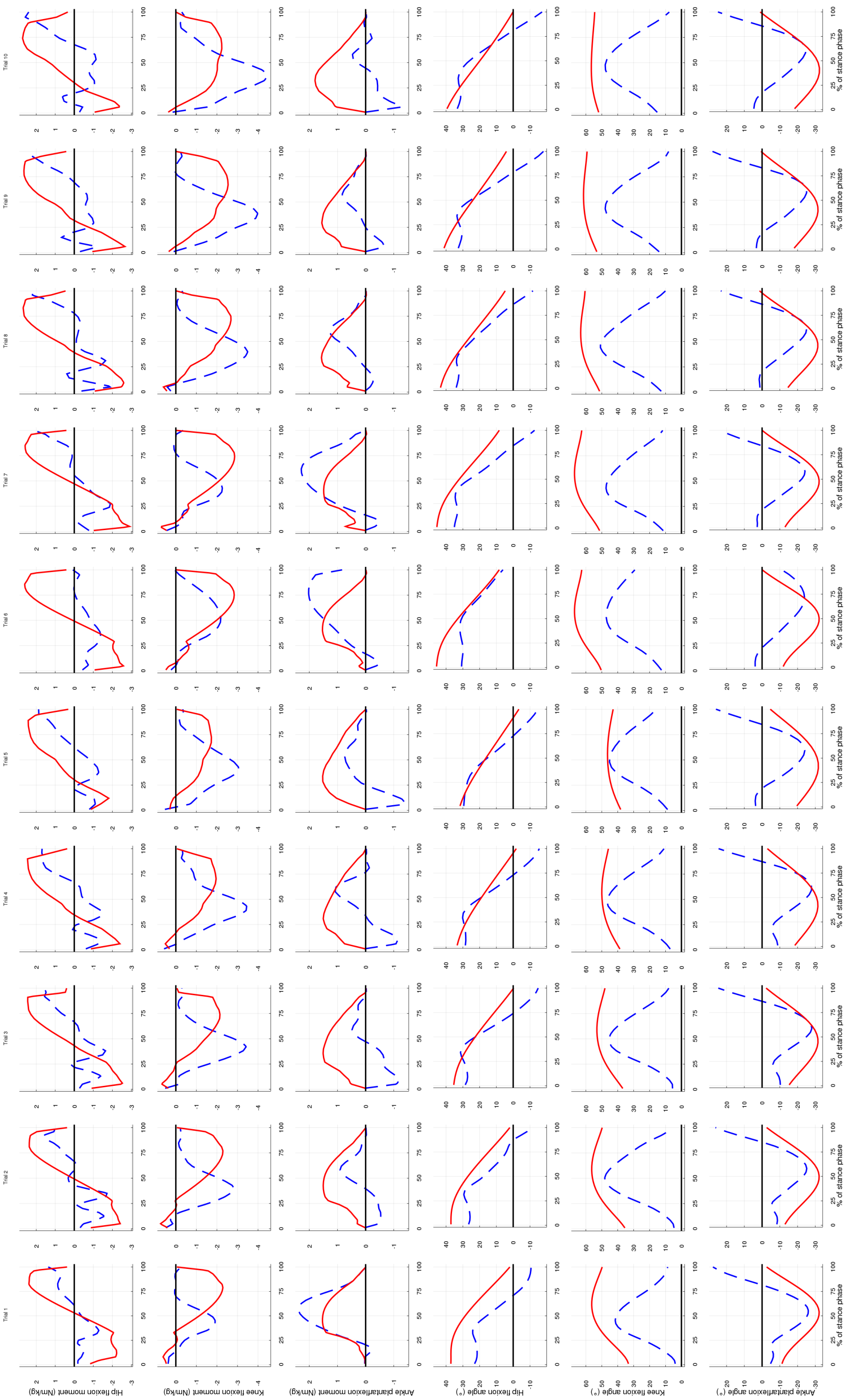

Figure 5.: Comparison of simulation results obtained with the SINGLE objective (red solid) and measurements (blue dashed). Each column contains one trial and each row contains one parameter.

Appendix 5: MATCHED-simulations vs measurements

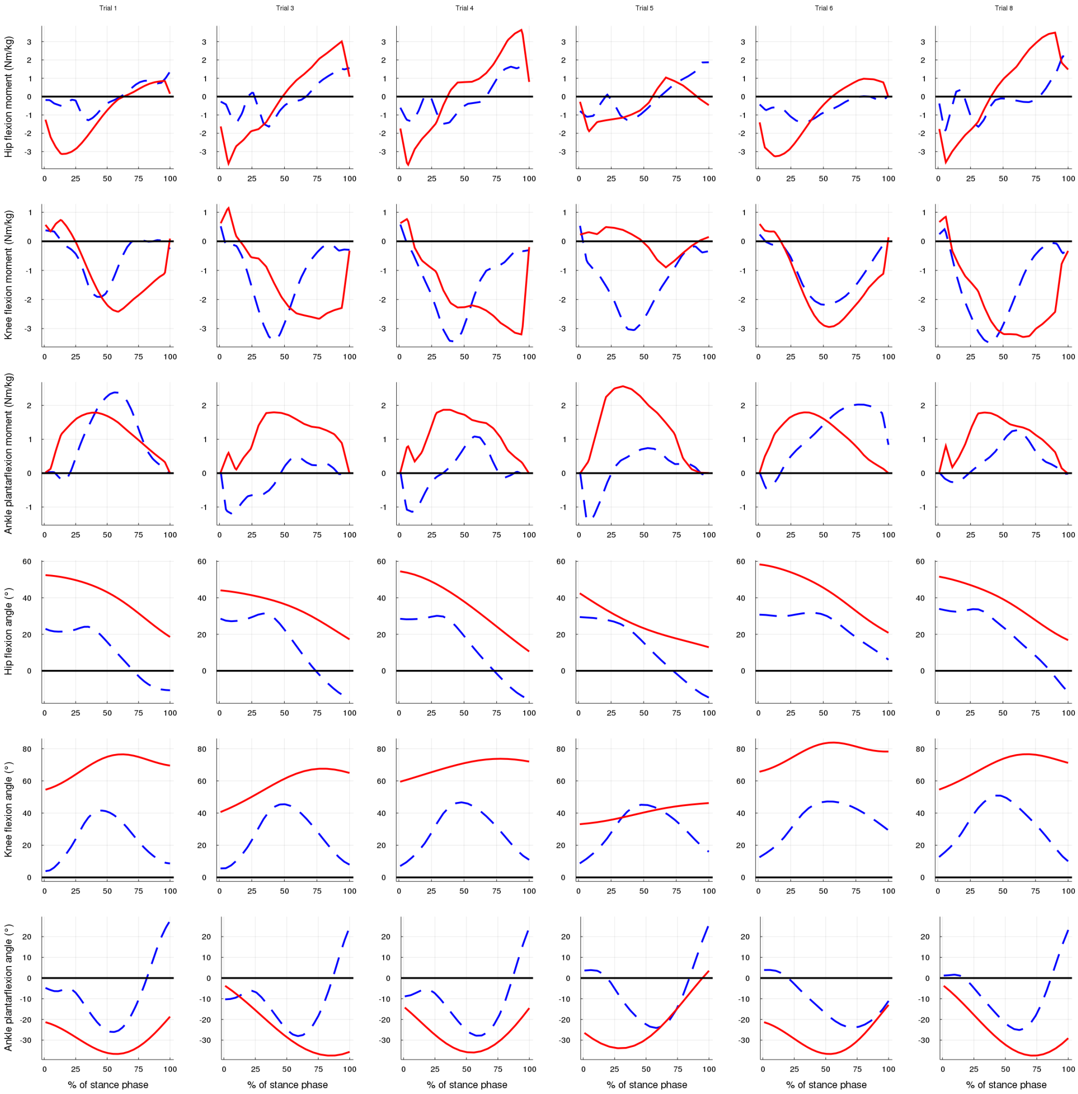

Figure 6.: Comparison of simulation results obtained with the MATCHED objective (red solid) and measurements (blue dashed). Each column contains one trial and each row contains one parameter.

Appendix 6: Correlation coefficients for training set

Measure	MINIMAL	COMZ	ANTHROPOMETRY	SINGLE	MATCHED
Hip flexion moment	0.64 [0.07; 0.76]	0.56 [-0.53; 0.81]	0.67 [0.58; 0.76]	0.65 [0.21; 0.86]	0.72 [0.57; 0.79]
Knee flexion moment	0.53 [-0.41; 0.93]	0.40 [-0.10; 0.69]	0.25 [0.25; 0.25]	0.13 [-0.08; 0.63]	0.30 [-0.20; 0.96]
Ankle plantarflexion moment	0.25 [-0.55; 0.68]	0.07 [-0.48; 0.88]	0.48 [0.09; 0.86]	0.25 [-0.24; 0.95]	0.57 [-0.19; 0.64]
Hip flexion angle	0.98 [0.93; 0.99]	0.97 [0.88; 0.99]	0.89 [0.80; 0.98]	0.97 [0.93; 0.99]	0.98 [0.93; 0.99]
Knee flexion angle	0.82 [-0.11; 1.00]	0.75 [-0.77; 0.93]	0.07 [-0.70; 0.85]	0.81 [0.57; 0.98]	0.43 [0.31; 0.98]
Ankle plantarflexion angle	0.56 [0.33; 0.96]	0.71 [-0.56; 0.99]	0.61 [0.49; 0.73]	0.79 [0.20; 0.93]	0.48 [-0.01; 0.84]

Table 5.: Median and range of correlation coefficients (r) for the five candidate objectives.

Appendix 7: Simulation vs measurements in validation set

Attached image file compares of simulation results (red solid) and measurements (blue dashed) for the validation set. Each column contains one trial and each row contains one parameter.

Appendix 8: Setup of optimization in Julia

The optimization procedure was setup and implemented in the Julia programming language (https://julialang.org/). The following Julia packages were used: MultivariateStats.jl (for performing PCA), Optim.jl (for the implementation of particle swarm optimization), CSV.jl (for reading CSV-files), DataFrames.jl (for utilities for handling data), GLM.jl (for constructing linear models). The code necessary for settting up the optimization can be found as an attached zip-file.